DMSP SSM/I-SSMIS Daily Polar Gridded Brightness Temperatures, Version 4

USER GUIDE

How to Cite These Data

As a condition of using these data, you must include a citation:

Maslanik, J. and J. Stroeve. 2004. *DMSP SSM/I-SSMIS Daily Polar Gridded Brightness Temperatures, Version 4*. [Indicate subset used]. Boulder, Colorado USA. NASA National Snow and Ice Data Center Distributed Active Archive Center. https://doi.org/10.5067/AN9AI8EO7PX0. [Date Accessed].

FOR QUESTIONS ABOUT THESE DATA, CONTACT NSIDC@NSIDC.ORG

FOR CURRENT INFORMATION, VISIT https://nsidc.org/data/NSIDC-0001

National Snow and Ice Data Center

TABLE OF CONTENTS

1 DETAILED DATA DESCRIPTION

Passive microwave observations of polar oceans have become essential to tracking the ice edge, for estimating sea ice concentrations, and for classifying sea ice types. Global data, immediately practical for use in shipping and petroleum development activities, have broader implications from the standpoint of adding to the meteorological foundations used in understanding and modeling climate change.

NSIDC produces daily gridded brightness temperatures from orbital swath data generated by the Special Sensor Microwave/Imager (SSM/I) aboard the Defense Meteorological Satellite Program (DMSP) F8, F11, and F13 platforms and the Special Sensor Microwave Imager/Sounder (SSMIS) aboard DMSP-F17. The SSM/I and SSMIS channels used to calculate brightness temperatures include 19.3 GHz vertical and horizontal, 22.2 GHz vertical, 37.0 GHz vertical and horizontal, 85.5 GHz vertical and horizontal (on SSM/I), and 91.7 GHz vertical and horizontal (on SSMIS). Thus, a total of nine channels result from vertical and horizontal polarization for each of five frequencies, with the exception of 22.2 GHz, which is vertical only. Data at 85.5 GHz and 91.7 GHz are gridded at a resolution of 12.5 km, with all other frequencies at a resolution of 25 km.

1.1 Format

Data are stored as scaled 2-byte integers in flat binary arrays. Byte order is little-endian. A factor of ten is applied to the brightness temperature value prior to converting the value to an integer. For example, a stored integer value of 2358 represents a brightness temperature value of 235.8 kelvins (K). A value of 0 represents missing data.

1.2 File Naming Convention

This section explains the file naming convention used for this product with an example.

Example File Name: `tb_f13_20000115_v2_n19v.bin`

`tb_fSS_YYYYMMDD_vV_RFFP.bin`

Refer to Table 1 for the valid values for the file name variables listed above.

Table 1. File Naming Convention Description

Variable	Description
tb	Identifies this as a file containing brightness temperatures
fSS	Sensor (f08, f11, f13, or F17)
YYYY	4-digit year
MM	2-character month
DD	2-digit day
vV	Data version number (example: v2)
R	Region (n: north; s: south)
FF	Frequency in GHz (19, 22, 37, 85, or 91)
P	Polarization (v: vertical, h: horizontal)

For example, `tb_f13_20000115_v2_n19v.bin` is a brightness temperature file for sensor F13, for the date 15 January 2000; it is Version 2 data for the north region and the 19.3 GHz vertical channel (the channel is the frequency and polarization).

1.3 File Size

The file size varies depending on the region and frequency, as shown in Table 2.

Table 2. File Size

Region	Channels	Size
North	85.5 and 91.7 GHz	1089536 Bytes
North	all others	272384 Bytes
South	85.5 and 91.7 GHz	839296 Bytes
South	all others	209824 Bytes

1.4 Spatial Coverage

Instrument coverage is global except for circular sectors centered over the pole, 311 km in radius, located poleward of 87.2° N and 87° S, which are never measured due to orbit inclination. Data set coverage includes the polar regions defined on the Polar Stereo web page. The measurement footprint size or effective field of view (FOV) is described in Table 3.

Table 3. Effective Field of View per Channel

Channel	FOV
19.3 GHz	70x45 km
22.2 GHz	60x40 km
37.0 GHz	38x30 km
85.5 GHz	16x14 km
91.7 GHz	16x13 km

1.4.1 SSM/I A/B Scan Geometry

Swath data consist of A/B scan pairs. Each pair includes 256 scene stations (numbered). Scene station numbers (parameter position numbers) are shown in Figure 1. Large circles signify all channels, and small circles signify high frequency channels. Brackets indicate scene stations lost due to antenna pattern correction.

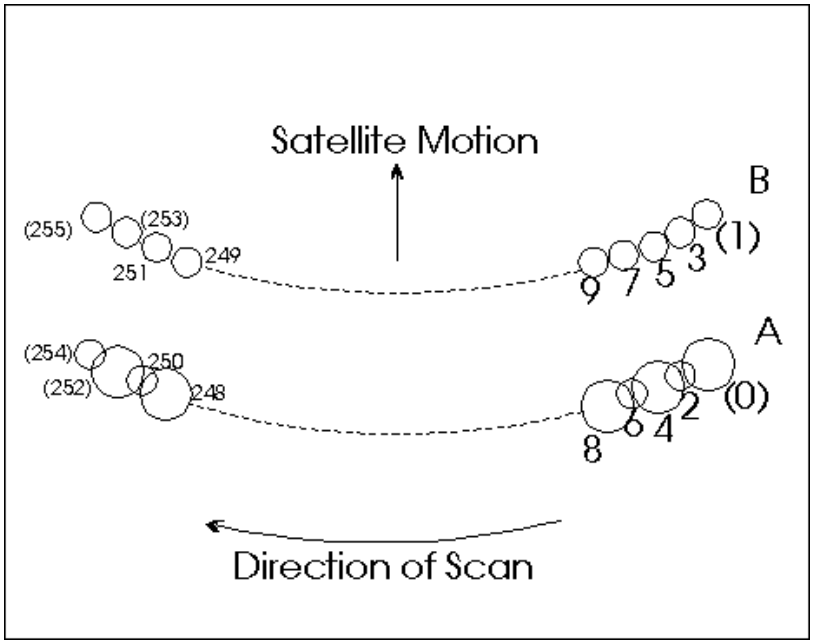

Figure 1. Parameter Position Numbers

1.4.2 Projection and Grid Description

The gridded brightness temperature data are displayed in polar stereographic projection. For more information, see Polar Stereo. The grid size varies depending on the region and frequency, as shown in Table 4.

Table 4. Grid Size by Region and Frequency

Region	Frequency	Columns	Rows
North	85.5 GHz or 91.7 GHz	608	896
North	all others	304	448
South	85.5 GHz or 91.7 GHz	632	664
South	all others	316	332

1.5 Temporal Coverage

Daily-averaged data begin 09 July 1987; processing of data for the F17 platform is ongoing. The brightness temperature data are averaged daily using the drop-in-the-bucket method.

Note to users of SSM/I polar stereographic data for 1994 through April 1995:

Substantial amounts of swath data over Alaska and the Canadian Prairies are missing beginning early in 1994 until May 1995. During this period the data tape recorder on the DMSP-F11 failed. As a result, it was necessary to download data to ground stations more frequently than usual. Data download and acquisition could not occur simultaneously; consequently, data gaps exist in the SSM/I data for Alaska and the Canadian Prairies from early 1994 until data acquisition by the DMSP-F13 SSM/I began in May 1995.

1.6 Parameter or Variable

1.6.1 Parameter Description

Brightness temperature is the effective temperature of a blackbody radiating the same amount of energy per unit area at the same wavelength as the observed body. This is also called effective temperature. Brightness temperatures are measured in kelvins (K).

Brightness temperatures are calculated at the following channels: 19.3V, 19.3H, 22.2V, 37.0V, 37.0H, 85.5V, 85.5H, 91.7V, and 91.7H. Nine channels result from vertical and horizontal polarization for each frequency, except 22.2 GHz, which is vertical only. Brightness temperature values are precise to 0.01 K.

1.6.2 Parameter Source

The parameter source is the Special Sensor Microwave/Imager (SSM/I) mounted on the Defense Meteorological Satellite Program (DMSP) F8, F11, and F13 platforms, and the Special Sensor Microwave Imager/Sounder (SSMIS) mounted on DMSP-F17.

1.6.3 Parameter Range

Data are stored as scaled 2-byte integers representing brightness temperature values (in tenths of a kelvin), ranging from 50 K to 350 K. A factor of ten is applied to the brightness temperature value prior to converting the value to an integer. For example, a stored integer value of 2358 represents a brightness temperature value of 235.8 K. A value of 0 represents missing data.

2 SOFTWARE AND TOOLS

2.1 Software and Tools

Tools for reading and displaying the brightness temperature files are available via FTP. Included are tools to extract the files; determine geolocation (geocoordinates) of data; display, extract and export the data; and masking tools that limit the influence of non-sea ice brightness temperatures.

The tools are divided into directories on the FTP site as shown in Figure 2.

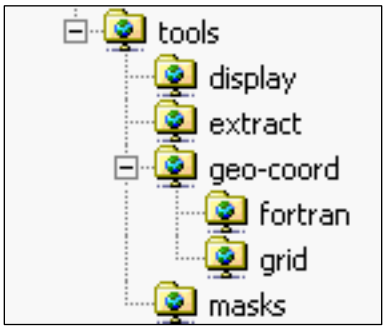

Figure 2. Tools Directory Structure

Table 5 lists the tools that can be used with this data set. For a comprehensive list of all polar stereographic tools and for more information, see the Polar Stereo web page.

Table 5. Tools for this Data Set

Tool Type	Tool File Name
Data Extraction	extract.pro
Data Display	display_ssmi_xa.pro
Geocoordinate	locate.for
	mapll.for and mapxy.for
	psn12lats_v3.dat and pss12lats_v3.dat
	psn12lons_v3.dat and pss12lons_v3.dat
	psn25lats_v3.dat and pss25lats_v3.dat
	psn25lons_v3.dat and pss25lons_v3.dat

Tool Type	Tool File Name
Pixel-Area	psn12area_v3.dat and pss12area_v3.dat
	psn25area_v3.dat and pss25area_v3.dat
Land Masks	gsfc_12n.msk and gsfc_12s.msk
	gsfc_25n.msk and gsfc_25s.msk
Land Overlays	coast_12n.msk and coast_12s.msk
	coast_25n.msk and coast_25s.msk
	ltln_12n.msk and ltln_12s.msk
	ltln_25n.msk and ltln_25s.msk

2.2 Quality Assessment

Beginning with January 2000, processing of brightness temperature data was modified to include two additional quality control steps. The first performs a statistical analysis on the brightness temperature data to look for possible calibration errors. The second was an along-scan adjustment that corrects for interference by the cold-space reflector at scans of 100 or greater, and the difference between antenna temperature observations and the Wentz radiative transfer model. Corrections can be as large as one kelvin. See Stroeve 1998 for more details. Brightness temperature data that included these additional quality control steps are only available for dates after January 2000.

3 DATA ACQUISITION AND PROCESSING

3.1 Theory of Measurements

The microwave radiometer measures the emitted energy from the earth/atmosphere system in the microwave wavelength region (1-100 GHz). The Rayleigh-Jeans approximation (Equation 2) can be used since it is a good approximation for the microwave region.

Equation 2 shows the Rayleigh-Jeans approximation equation and is described in Table 6.

$E_\lambda = 2kcT/\lambda^4$ **(Equation 2)**

Table 6. Rayleigh-Jeans Equation Description

Variable	Description
E_λ	Emittance as a function of wavelength
k	Boltzmann's constant (1.38 x 10-23 J K-1)
c	Speed of light (3 x 108 ms-1)
T	Temperature in kelvins
λ	Wavelength

3.1.1 Processing History

Table 7 outlines the processing and algorithm history for this product.

Table 7. Description of Processing Changes

Data Version	Sensor	Temporal Range	Source Data Version	Description of Changes
V4	F17	14 Dec 2006 – 02 October 2018	RSS V7	• Updated version to reflect the beginning of the F17 data record • The source for this data set, RSS, changed from their version from V4 to V7 • RSS V7 cross-calibrates between all SSM/I and SSMIS sensors as well as AMSR-E and WindSat, providing interconsistency of brightness temperatures from the sensors
V3	F13	01 July 2008 – 29 Apr 2009	RSS V6	Updated to include additional inter-sensor calibrations
V2	F13	03 May 1995 – 30 Jul 2008	RSS V4	Updated version to reflect the beginning of the F13 data record
V2	F11	03 Dec 1991 – 30 Sep 1995	RSS V3	N/A
V2	F8	09 Jul 1987 – 31 Dec 1991	RSS V3	N/A
V1	F8	Not available	N/A	Original version of data. Note: V01 was not indicated in Version 1 file names.

3.2 Data Acquisition Methods

Both the SSM/I and SSMIS instruments rotate continuously about an axis parallel to the local spacecraft vertical and measure the upwelling scene brightness temperatures. The absolute brightness temperature of the scene incident upon the antenna is received and spatially filtered by the antenna to produce an effective input signal, or antenna temperature, at the input of the feed horn antenna. The passive microwave radiometer output voltages are transmitted to both the Air Force Global Weather Central (AFGWC) at Offutt Air Force Base, Nebraska and the FNMOC in Monterey, California.

At both locations, the radiometer output voltages are converted to sensor counts. The AFGWC sensor counts are relayed to the National Environmental Satellite, Data, and Information Service (NESDIS), reformatted into the NESDIS Level-1B format, and used by NESDIS in generating temperature sounding data sets from another instrument. FNMOC converts their sensor counts into antenna temperature Temperature Data Records (TDRs), brightness temperature Sensor Data Records (SDRs), and derived geophysical parameters from Environmental Data Records (EDRs). The TDRs, SDRs, and EDRs are sent to NESDIS for archival. The FNMOC antenna temperatures are used as the basis for the SSM/I antenna temperatures and geophysical parameter data sets produced by RSS.

3.2.1 Difference Between SSM/I and SSMIS High Frequency Channels

Regarding F17 data, users should note a difference in the high frequency channel. The SSMIS sensor is similar to the SSM/I sensor and has the same low frequency channels: dual-polarized 19 GHz and 37 GHz channels, and a vertically polarized 22 GHz channel. However, the high frequency 85.5 GHz channel on SSM/I has been replaced by a 91.7 GHz channel on SSMIS. Users should note that the different frequency will affect any products that employ a high frequency channel. Any such products should be evaluated for the impact of the different frequency and adjustments may be necessary for consistenty between products.

3.3 Data Source

In the initial years of processing (09 July 1987 to 05 October 1988), NSIDC obtained SSM/I F8 data from the NOAA/National Environmental Satellite Data and Information Service (NESDIS) Satellite Data Services Division (SDSD), which is the primary archive of DMSP SSM/I data in Level-1B orbital format. The data consisted of TDR files produced by the FNMOC as part of their operational data processing. These data were sent by FNMOC to SDSD and then to NSIDC. TDR files contain Earth-located antenna temperatures and sensor calibration data.

After 05 October 1988, SSM/I data were obtained from Remote Sensing Systems, Inc. (RSS) in Santa Rosa, California USA. The SSM/I data obtained by RSS are DEF tapes produced by FNMOC. RSS ingests the DEF tapes and organizes the data into a chronological, orbit-by-orbit data set (Wentz 1993).

No modifications of the DEF antenna temperatures and calibration data are performed; however, errors were discovered in the cell latitude and longitudes; therefore, for data starting 01 January 1989, cell latitudes and longitudes are computed from a smoothed orbit ephemeris rather than using the DEF values. Fortunately, except for a brief period during the second half of February 1988, no large errors in the ephemeris prior to 1989 have been found.

Tapes received by NSIDC from RSS contain antenna temperatures along with sensor calibration data. Prior to 01 January 1989, the tapes contain DEF latitudes and longitudes, and after 01 January 1989, the antenna temperatures are geolocated. RSS provides software to convert antenna temperatures to brightness temperatures.

3.3.1 Data Source Version Change

Remote Sensing Systems (RSS), the source for NSIDC gridded brightness temperature data, released a new version of their product to accommodate the release of F17 data: Version 7 (V7). NSIDC was previously using RSS Version 4 (V4) data from the DMSP-F13 satellite. To ensure the highest level of quality and consistency across DMSP data, NSIDC distributes V4-derived data from the beginning of the F13 satellite record through the last day of reliable and complete F13 data, 03 May 1995 through 31 December 2007, respectively. V7-derived data are distributed from the beginning of the F17 satellite record, 14 December 2006, onward.

To reflect the beginning of the F17 data record and RSS version change to V7, NSIDC has revised the version number of its gridded brightness temperature product from V3 to V4. Table 8 lists the temporal coverage by satellite and the corresponding product version numbers for this data set.

Table 8. Temporal Coverage and Data Versions for DMSP Brightness Temperature Data

DMSP Satellite	Temporal Coverage	RSS Version	NSIDC Version
F8	09 July 1987 - 31 December 1991	V3	V2
F11	03 December 1991 - 30 September 1995	V3	V2
F13	03 May 1995 - 31 December 2007	V4	V3
F17	14 December 2006 - 02 October 2018	V7	V4

Intercomparison of F13 and F17 Data

NSIDC conducted an intercomparison of F13 with F17 data during the 01 January 2007 through 31 December 2007 time period. The vast majority of differences are between 0.5 K and 2 K. Some

larger differences, up to 10 K, are found primarily in regions of sharp gradients of brightness temperatures, along coasts and the ice edge, likely due to the changes in geolocation. Smaller biases of 0.5 K to 2 K in some channels, such as 19V, 19H, 22V, and 37H, are likely due to the cross-sensor calibration.

3.4 Derivation Techniques and Algorithms

3.4.1 Processing Steps

3.4.1.1 Processing for F8 Gridded Brightness Temperatures

F8 Temperature Data Records (TDRs) are loaded into an Input Copy Archive (ICA) at NSIDC. The ICA consists of two types of records: file header and scan pair data records. The following parameters are copied directly from the TDR file to the ICA file header record:

- Product identifier
- Product generation year, month, day, hour, and minute
- Revolution/orbit number
- Data day, hour, minute, and second

The archive calculates the year that the data begin and specifies an antenna pattern correction algorithm to convert the antenna temperatures to brightness temperatures.

Latitudes, longitudes, and position numbers are copied from the SSM/I TDR file to the ICA scan pair data record. The archive converts the time into seconds past 01 January 1950.

Antenna temperatures are converted to brightness temperatures by applying an antenna pattern correction (see below for a description of this correction). Next, data are entered into the Rapid Access Archive (RAA) in a format accessible by the NSIDC archive system. Data are then extracted from the RAA and used to create the level 3 grid product. The first two level 3 archives (3A and 3B) are of gridded brightness temperatures.

3.4.1.2 Processing for F11 and F13 Brightness Temperatures

Processing for F11 and F13 data involves transferring the 8 mm data tapes from RSS to an optical jukebox system. The DECODE algorithm (Wentz 1991) decodes the information on the antenna temperature tapes and applies corrections before converting them to brightness temperatures. For the F8 satellite, an along-scan adjustment corrects for the scan error that occurs near the edge of the scan where the feed horn partially sees the cold-sky reflector. For the F11 and F13 satellites, no correction for the along-scan error is made, since at the time of production, the along-scan adjustments were not available.

Beginning with January 2000, processing of brightness temperature data was modified to include two additional quality control steps. The first performs a statistical analysis on the brightness temperature data to look for possible calibration errors. The second was an along-scan adjustment which corrects for interference by the cold-space reflector at scans of 100 or greater, and the difference between antenna temperature observations and the Wentz radiative transfer model. Corrections can be as large as 1 K. See Stroeve (1998) for more details. Brightness temperature data that included these additional quality control steps are only available for dates after January 2000.

3.4.1.3 Antenna Pattern Correction

Since 05 October 1988, SSM/I brightness temperatures also reflect an antenna pattern correction algorithm provided by RSS. See Wentz (1993) for information for information. Prior to 05 October 1988, the antenna pattern correction was supplied by FNMOC. Quality control procedures are carried out before further processing.

3.4.1.4 Reprocessing for Scan Errors in 1987-1999 Data

July 2006

Recent investigation revealed that errors in some daily SSM/I brightness temperature fields prior to 2000 (Molthan and Anderson, 2005) were not properly flagged and therefore were considered good data by our processing software. These brightness temperature errors were generally 5-15 K, but could be as high as 20 K. These errors were usually found in groups of pixels constituting a scan about 60 pixels in length and 1 or 2 pixels wide. The bad scans do not appear in all daily data. They were most prevalent during spring and summer (1 March – 30 September) 1989, during which time the 19H grids had 67 days (28%) with bad values and the 37H grids had 51 days (21%) with bad values. Bad scans sometimes occurred in multiple channels on the same day and could also be collocated or partially overlapping.

NSIDC determined that the version of the processing software used before 2000 failed to account for these bad scans and flag them. Updated software implemented in 2000 corrected this problem from that point forward. However, the 1987-1999 brightness temperatures contain the bad scans, so in 2006 we reprocessed the 1987-1999 data using the updated software to remove the bad scans. The entire data set, including this reprocessed data, was released as Version 2 in July 2006. Version 2 also includes the conversion of all data from HDF to 2-byte flat binary, and a new file naming convention.

These errors can lead to errors in derived data, such as sea ice concentrations. Averaged products (e.g., monthly means or polar basin-scale) are not likely to be significantly impacted, but daily sea

ice concentration fields may show a signature from the bad brightness temperatures. NSIDC plans to reprocess our sea ice concentrations data in the future.

3.4.1.5 Processing for F17 Brightness Temperatures

RSS processing steps for F17 brightness temperatures include the following:

1. SSMIS TDRs are reverse engineered back to the raw telemetry data.
2. The raw counts are processed to brightness temperatures using a standard set of proven algorithms.
3. A number of adjustments and corrections are then applied to the brightness temperature data to achieve full calibration, including:
    a. Adjustments to the SSMIS pointing angles to achieve proper geolocation.
    b. Corrections to remove the effects of the SSMIS emissive antenna (which affects all SSMIS channels).
    c. Corrections to remove the Moon intrusion into the cold mirror.
    d. Corrections to remove the Sun intrusion into the hot load.
    e. Flagging of anomalous jumps in the radiometer counts.
    f. Application of extensive quality control with respect to geolocation information and radiometer performance.
    g. Adjustments to the antenna pattern coefficients to provide precise (0.1K or better) inter-calibration with all other microwave imagers.

3.4.2 Error Sources

3.4.2.1 F17 Solar Panel Position Shift

On 5 April 2016, the solar panel on the F17 Satellite shifted position compromising the integrity of Channel 16 (37Ghz vertical polarization). On 25 May 2016, a fix was implemented, however, the long term quality of the data is still unknown. NSIDC continues to monitor the quality of the data.

3.4.2.2 Geolocation Errors

Geolocation is a continuing problem for users of the SSM/I passive microwave data. Shortly after the SSM/I Temperature Data Records (TDRs) were released by the Fleet Numerical Meteorology and Oceanography Center (FNMOC), independent investigations at the University of Massachusetts and at NSIDC determined that geolocation for the sensor was inaccurate. In addition, while processing the 1988 SSM/I data, Remote Sensing Systems (RSS) found a number of problems with the spacecraft and Earth locations computed at FNMOC, causing errors in excess of 20 to 30 km in the SSM/I data. Latitudes and longitudes on the Data Exchange Format (DEF) tapes produced by FNMOC were in error due to the following problems. Refer to Wentz 1993 for more details:

- There are some algorithm errors in the FNMOC data processing software. FNMOC and its contractors are continuing to improve their operational software.
- The satellite ephemeris is sometimes incorrect due to spacecraft tracking errors and orbit prediction errors. This problem is particularly severe during periods of increased solar activity.
- The bore site nadir angle and the alignment of the SSM/I instrument relative to the spacecraft are slightly misspecified.

In response to the problems identified, RSS developed a routine for computing the latitude and longitude rather than using the DEF values. The input to their geolocation routine is the satellite ephemeris for approximately a seven-day period centered on the processed orbit. The ephemeris is first subjected to quality control and then smoothed to remove any noise. The smoothed ephemeris is then used to compute the SSM/I cell latitudes and longitudes. This algorithm is believed to improve the geolocation accuracy to within 5 km (Wentz, personal communication).

The Wentz procedure of computing latitude and longitude from a smoothed ephemeris was initiated with the 1 January 1989, F8 antenna temperature tape. For data collected prior to 1989, a correction algorithm (Equation 1) developed by researchers at the University of Massachusetts' Department of Electrical and Computer Engineering was used. This results in location accuracies within approximately 8 km both along and across the scan (Goodberlet 1990). The algorithm assumes all geolocation errors are a result of the pitch, yaw, and roll of the satellite. The three attitude angles were found to have latitude and time dependencies.

Equation 1 shows the algorithm used for data collected before 15 May 1988 and is described in Table 9.

$$angle = C_1 + C_2*JDAY + C_3*abs(LAT) + (C_4*JDAY^2)/10000 \quad \textbf{(Equation 1)}$$

Table 9. Correction Algorithm Description

Variable	Description
C1, C2, C3, C4	Constants
angle	Pitch, yaw, or roll correction angle in degrees
JDAY	Number of days since the beginning of 1987
LAT	Scene latitude in degrees

3.4.2.3 Bad Data Value in Some 1987-1988 Data

During the early stages of the SSM/I archival effort, some of the data from the F8 TDR tapes, covering 09 July 1987 through 05 October 1988, fell outside the realistic range expected for brightness temperatures derived from the microwave sensor. Statistically, SSM/I brightness temperatures should fall between 50 K and 350 K.

An editing procedure, developed by the NASA Ocean Data System archiving development team, is applied to these data to flag and edit records containing out-of-range values. Using the 19.3 GHz frequency, one SSM/I footprint per scan is analyzed. The scan is suspect if the value of this footprint is out of normal bounds. Should 20 or more scans be flagged in a given TDR file, the footprint is plotted against the local time of the orbital pass, and time ranges of suspect data are deleted from the Input Copy Archive (ICA) prior to swath (Rapid Access Archive, RAA) loading.

The 85.5 GHz channel is considered experimental because a passive microwave sensor with 12.5 km resolution has never before been deployed on an orbital scanner. Therefore, this channel is not used in this analysis. The SSM/I Sea Ice Algorithm Working Team (SSIAWT) decided to retain as many of these data records as possible, despite the anomalies that will be observed within the 85.5 GHz grids.

F11 antenna temperature values are sometimes completely unphysical, ranging from 0 K to 650 K. The cause for this is unclear, but telemetry errors are suspected. Data less than 50 K and greater than 350 K are flagged and not processed.

The antenna temperatures from RSS are also quality controlled for bad data values. For the F8 data, RSS inspects the data for two types of erroneous data:

- Observation time is sometimes in error; in this case, the antenna temperature values are correct, but the latitudes and longitudes are in error.
- Antenna temperature values are outside a realistic range.

Both types of erroneous data usually occur over a complete DEF data file and are detected by visually inspecting the data. A small American Standard Code for Information Interchange (ASCII) data file that contains the periods of erroneous data is included with the RSS antenna temperature tapes.

The F11 data have additional quality control, where a flag is set for the following conditions:

- The scan time is within an erroneous data time period.
- The calibration data for the scan is erroneous.
- The scan is within a group of 10 scans that has erroneous calibration data.

The antenna temperature value is outside the range of possible Earth values. See the Wentz (1993) for a complete description of the above errors.

3.4.2.4 Problems with 85.5 GHz Channel Data

85.5 GHz data from 1991 were of considerably poor quality; thus, they were not distributed with F8 data. Hardware temperatures aboard the F8 platform went through significant heating cycles every winter, due to increased solar illumination, which resulted in degradation of 85.5V and 85.5H

channels. In December 1987, the 85.5V temperature resolution began to degrade. After April 1988, the noise in the 85V channel exceeded 20 K. Between May 1988 and January 1989, there were windows of noise subsidence, so useful information was sporadic. However, after January 1989, the large noise increase rendered the 85.5H channel useless. During the first heating cycle, the 85.5H channel showed a slight degradation in temperature resolution, but recovered. The second heating cycle in December 1988 seemed to cause a small permanent degradation, while the third heating cycle damaged this channel, and resulted in a noise increase of 5-10 K. After January 1991, the noise exceeded 20 K (Wentz 1991); thus, 85.5 GHz data for 1991 were not distributed.

3.4.2.5 Latitude, Longitude, and Pixel Area File Errors, Corrected 1999

In summer 1999, NSIDC was alerted to errors in latitude, longitude, and pixel area files supplied with SSM/I polar stereographic gridded data.

Also refer to Molthan and Anderson (2005) for information on bad scans in some brightness temperature fields, and see section Reprocessing for Scan Errors in 1987-1999 Data for information about the release of reprocessed data.

3.4.2.6 Filter Error in Some 1990-1992 Data, Corrected 2006

NSIDC determined that a required filter to remove incorrectly calibrated brightness temperatures was not used, affecting some data files in the two-year period from 01 October 1990 to 30 September 1992. This problem was corrected, and data for the period from 01 October 1990 to 30 September 1992 were reprocessed. The corrected files were staged on the FTP site on 26 September 2006.

3.4.2.7 Removal of Some F13 Data

Problems with the aging F13 satellite began in early 2008. Thus, to ensure the highest level of quality and consistency across DMSP data, NSIDC will only distribute F13-derived data from the beginning of the F13 satellite record through the last day of reliable and complete F13 data, 03 May 1995 through 31 December 2007, respectively. NSIDC advises data users to exercise caution when using previously obtained F13 data with temporal coverage later than 31 December 2007.

3.5 Sensor or Instrument Description

The instruments used to acquire this data set are the SSM/I instruments on the Defense Meteorological Satellite Program (DMSP) F8, F11, and F13 satellites, and the Special Sensor Microwave Imager/Sounder (SSMIS) instrument on DMSP-F17.

The SSM/I instrument is a seven-channel, four-frequency, orthogonally polarized, passive microwave radiometric system. The instrument measures combined atmosphere and surface radiances at 19.3 GHz, 22.2 GHz, 37.0 GHz and 85.5 GHz. Please see the SMMR, SSM/I, and SSMIS Sensors Summary for more details.

The SSMIS sensor is a conically-scanning passive microwave radiometer that harnesses the imaging and sounding capabilities of three previous DMSP microwave sensors, including the SSMI, the SSM/T-1 temperature sounder, and the SSMI/T-2 moisture sounder. The SSMIS sensor measures microwave energy at 24 frequencies from 19 to 183 GHz with a swath width of 1700 km. Please refer to the SMMR, SSM/I, and SSMIS Sensors Summary for more details.

Table 10 compares the orbital parameters for each DMSP satellite.

Table 10. Comparison of Orbital Parameters: DMSP-F8, DMSP-F11, DMSP-F13, and DMSP-F17

Parameter	DMSP-F8	DMSP-F11	DMSP-F13	DMSP-F17
Nominal Altitude	860 km	830 km	850 km	850 km
Inclination Angle	98.8°	98.8°	98.8°	98.8°
Orbital Period	102 minutes	101 minutes	102 minutes	102 minutes
Ascending Node Equatorial Crossing (Local Time)	~6:00 a.m.	~5:00 p.m.	~5:45 p.m.	~5:31 p.m.

3.5.1 Sensor/Instrument Measurement Geometry

The following text is adapted from Hollinger and Lo 1983, pp. 1-3:

The SSM/I instrument consists of a 24 inch x 26 inch offset parabolic reflector fed by a corrugated, broad-band, seven-port horn antenna. The reflector and feed are mounted on a drum which contains the radiometers, digital data subsystem, mechanical scanning subsystem, and power subsystem.

The reflector-feed drum assembly is rotated about the axis of the drum by a coaxially mounted bearing and power transfer assembly (BAPTA). All data, commands, timing and telemetry signals, and power pass through the BAPTA on slip ring connectors to the rotating assembly.

The SSM/I rotates at a uniform rate making one revolution in 1.9 seconds, during which the satellite advances 12.5 km. The antenna beams are at an angle of 45° to the BAPTA rotational axis, which is normal to the earth's surface; thus, as the antenna rotates, the beams define the surface of a cone, and, from the orbital altitude of 833 km, make an angle of incidence of 53.1° at the earth's surface.

The scene is viewed over a scan angle of 102.4° centered on the ground track aft of the satellite, resulting in a scene swath width of 1394 km. The radiometer outputs are sampled differently on alternate scans. During the scene portion of the scans (Type A) the five lower frequency channels are each sampled over 64 equal 1.6° intervals, and the two 85.5 GHz channels are each sampled over 128 equal 0.8° intervals, or approximately every 11 km along the scan. During the alternate scans (Type B), only the two 85.5 GHz channels are sampled, at 128 equal intervals.

Sampling to 12-bit precision is accomplished by the integrate, hold, and dump method, with an integration period of 7.95 milliseconds for the five lower frequency channels and an integration period of 3.89 milliseconds for the 85.5 GHz channels. Alternate 0.8° intervals are centered on the mid-points of the 1.6° intervals, so that samples of all seven channels are collected with additional 85.5 GHz samples equally spaced between them.

Thus, the five lower channels are sampled on an approximately 25 km grid along the scan and along the track. The two 85.5 GHz channels are sampled at one-half this spacing both across and along the track.

3.5.2 Manufacturer of Instrument

The Hughes Aircraft Company built the SSM/I instrument; the SSMIS instrument was built by GenCorp Aerojet under a subcontract from Northrup Grumman Electronic Systems.

3.5.3 Calibration

3.5.3.1 SSM/I Instrument

A small mirror and a hot reference absorber are mounted on the BAPTA and do not rotate with the drum assembly. They are positioned off-axis such that they pass between the feed horn and the parabolic reflector, occulting the feed once each scan. The mirror reflects cold sky radiation into the feed, thus serving, along with the hot reference absorber, as calibration references for the SSM/I. This scheme provides an overall absolute calibration that includes the feed horn. Corrections for spillover and antenna pattern effects from the parabolic reflector are incorporated in the data processing algorithms.

3.5.3.2 SSMIS Instrument

The following text is adapted from the 2002 Northrop Grumman Algorithm and Data User Manual (ADUM) for the Special Sensor Microwave Imager/Sounder (SSMIS):

The SSMIS measures microwave energy from the surface and atmosphere of the Earth with a rotating 24-inch parabolic reflector. This reflector then focuses the energy on an assembly of six

feedhorns, which provide the initial frequency multiplexing for the 24 channels. The reflector and the six feedhorns rotate with the entire sensor canister. Mounted at the top of the canister are a cold calibration reflector and a warm calibration source, which do not rotate with the canister. Thus, the feedhorns view a fixed, cold calibration reflector and a fixed, warm calibration source for each revolution of the sensor. The resulting calibration data are used to convert the sensor output to absolute radiometric brightness temperatures.

The feedhorn data are input to the receiver subsystem where frequency multiplexing occurs to produce 24 channels of data. Receiver channel characteristics are summarized in Section 2.2 of the ADUM for the SSMIS. The receiver outputs are converted to the video spectrum, digitized and formatted, and sent to the Operational Linescan System (OLS) under control of the sensor signal processor and the flight software. The SSMIS data are transmitted to the ground by the OLS. Ground processing is performed at Air Force Weather Agency (AFWA) and Fleet Numerical Meteorological Oceanography Center (FNMOC) to convert the sensor data into calibrated and Earth-located Sensor Data Records (SDRs), and finally into a variety of Environmental Data Records (EDRs). (Northrop Grumman 2002)

3.6 Calculated Variables

3.6.1 Calculation of the SSM/I Brightness Temperature Archive

(Courtesy Charles S. Morris, NASA/JPL)

Two archives of gridded brightness temperatures are maintained: one for the 85.5 GHz channels (the 3A archive), and one for the lower five channels (the 3B archive). The 3A and 3B archives of one-day average brightness temperatures are calculated from the SDR Rapid Access Archive, in which the SSM/I swath brightness temperatures are stored.

The swath data consist of A/B scan pairs. Each A/B scan pair includes 256 scene stations (numbered 0-255). The B scan has 128 scene stations that contain measurements of the horizontal and vertical 85.5 GHz channels. The A scan also has 128 scene stations, but these alternate between scene stations with all seven SSM/I channels and those with only the 85.5 GHz channels. For data prior to 5 October 1988, only 250 of the 256 scene stations in a SDR A/B scan contain valid data. The end scene stations are lost when the antenna temperatures are converted to brightness temperatures.

Swath data are binned on two grids. The 85.5 GHz data are binned to a 12.5 km grid (3A archive), while the 19.3 GHz, 22.2 GHz, and 37.0 GHz data are binned to a 25 km grid (3B archive).

The methodology for binning the swath brightness temperatures into the 12.5 km and 25 km grid cells has been carefully considered. Previous work (Nimbus-5 ESMR and Nimbus-7 SMMR) used a simple average (drop-in-the-bucket) approach where the grid cell that contained the center of the observation footprint was given the whole weight of the observation. After reviewing several alternatives to this method of binning, NSIDC concluded that the increase in accuracy obtained with more sophisticated algorithms was not sufficient to warrant increasing the required computer time for binning by a factor of 30 or more; thus, the drop-in-the-bucket approach was adopted. The ability to switch to a more sophisticated algorithm in the future has been retained by structuring the archive to accept a fractional number of observations. For the current binning procedure, the number of observations will always be whole numbers. All valid brightness temperature observations within the extent of the SSM/I polar grids are binned into grid cells that include observations over land.

Accordingly, swath data from each channel are mapped to the 12.5 km or 25 km north polar stereographic grid by converting the SSM/I geodetic latitude and longitude for the center of each scene station (observation footprint) into SSM/I map grid coordinates. Scene station map grid coordinates determine grid cell assignments. Observations falling outside the SSM/I grid are ignored. For each grid cell, brightness temperatures observed over a 24-hour period (midnight to midnight GMT) are summed, then divided by the total observations to obtain an average brightness temperature. If no observations fall within a grid cell, the average brightness temperature will be labeled missing.

3.6.2 Antenna Pattern Correction Algorithm

Antenna temperatures, which are calibrated sensor counts, are converted to brightness temperatures during creation of the Input Copy Archive by applying an antenna pattern correction. The correction algorithm applied to the SSM/I data from 9 July 1987 through 5 October 1988 is the same as that used by FNMOC to convert antenna temperatures into brightness temperatures. See Wentz (1993) for more information on the antenna pattern correction applied to files dated 5 October 1988 and beyond.

The brightness temperature at each scan position is calculated by a weighted sum of the antenna temperatures at central and near neighbor positions. Near neighbors may be in the same or neighboring scans. Brightness temperatures consist of seven separate frequency/polarization channels. Each channel uses a separate set of weighting coefficients for the antenna temperature to brightness temperature conversion. Weighting coefficients apply to antenna temperatures with the same frequencies as computed brightness temperatures, and they allow polarization mixing only at the central scan position. An exception occurs with the 22.2 GHz vertical brightness temperature, since the 22.2 GHz horizontal antenna temperature is missing and is approximated with a linear function of the 19.3 GHz horizontal antenna temperature. In addition, the antenna

scan is divided into five separate regions, each of which has a separate set of weighting coefficients for the seven channels.

Each set of weighting coefficients is associated with an explicit set of near neighbor positions; thus, the set of near neighbor positions can vary with brightness temperature channel and location within the antenna scan.

The antenna temperature to brightness temperature conversion is written as a large matrix equation, where the input vector corresponds to all the scans from a complete revolution stacked on top of each other. In principle, this matrix equation can be inverted.

Equation 3 shows the antenna pattern correction for the 19.3 GHz vertical, brightness temperature and is described in Table 11.

$$TB_{19V(i,j)} = C_1 * TA_{19V(i,j)} + C_2 * TA_{19H(i,j)} + C_3 * TA_{19V(i-n1,j)} + C_4 * TA_{19V(i+n1,j)} + C_5 * TA_{19V(i+n3,\ j+n2)} + C_6 * TA_{19V(i-n4,\ j-n2)} \quad \textbf{(Equation 3)}$$

Table 11. Antenna Pattern Correction for 19.3 GHz Vertical Brightness Temperature

Variables	Description
T_{B19V}	Brightness temperature for the 19 GHz, vertical channel
T_{A19V}	Antenna temperature for the 19 GHz, vertical channel
i	Position within a scan
j	Scan number
C_1, C_2, C_3, C_4, C_5, C_6	Weighting coefficients (sum = 1)
n1, n2, n3, n4	Position of near neighbors

4 REFERENCES AND RELATED PUBLICATIONS

Algorithm and Data User Manual (ADUM) for the Special Sensor Microwave Imager/Sounder (SSMIS). 2002. Northrop Grumman Corporation Space Systems Division. Technical Report 12621. Azusa, California USA.

Abdalati, W., K. Steffen, C. Otto, and K. C. Jezek. 1995. Comparison of Brightness Temperatures from SSM/I Instruments on the DMSP F8 and F11 Satellites for Antarctica and the Greenland Ice Sheet. International Journal of Remote Sensing 16(7):1223-1229.

Ackley, S. F. 1979. Mass Balance Aspects of Weddell Sea Pack Ice. Journal of Glaciology 24(90):391-406.

Ackley, S. F., A. J. Gow, K. R. Buck, and K. M. Golden. 1980. Sea Ice Studies in the Weddell Sea Aboard USCGC Polar Sea. Antarctic Journal of U. S. 15(5):84-86.

Bonbright, D. I. 1984. PODS SSM/I Functional Requirements (Version 1.0). Jet Propulsion Laboratory Document 715-63.

Bonbright, D. I., J. W. Brown, J. E. Hilland, I. T. Hsu, J. A. Johnson, T. L. Kotlarek, R. A. Lassanyi, C. L. Miller, C. S. Morris, and F. J. Salamone. 1987. NASA Ocean Data System Version 3.0. User handbook. Jet Propulsion Laboratory. Document 715-66, 50pp. + appendices.

Campbell, W. J., P. Gloersen, and H. J. Zwally. 1984. Aspects of Arctic Sea Ice Observable by Sequential Passive-microwave Observations from the Nimbus 5 Satellite. In Arctic technology and policy. I. Dyer and C. Chryssostomidis, eds. New York: Hemisphere Publishing. pp. 197-222.

Carsey, F. D. 1982. Arctic Sea Ice Distribution at End of Summer 1973-1976 from Satellite Microwave Data. Journal of Geophysical Research 87:5809-5835.

Cavalieri, D. J. and P. Gloersen. 1984. Determination of Sea Ice Parameters with the Nimbus 7 SMMR. Journal of Geophysical Research 89(D4):5355-5369.

Cavalieri, D. J., P. Gloersen, and W. J. Campbell. 1984. Determination of Sea Ice Parameters with the NIMBUS-7 SMMR. Journal of Geophysical Research 89(D4):5355-5369.

Cavalieri, D. J., P. Gloersen, and T. T. Wilheit. 1986. Aircraft and Satellite Passive Microwave Observations of the Bering Sea Cover During MIZEX West. IEEE Transactions on Geoscience and Remote Sensing GE-24:368-377.

Cavalieri, D. J., K. M. St. Germain, and C. T. Swift. 1995. Reduction of Weather Effects in the Calculation of Sea Ice Concentration with the DMSP SSM/I. Journal of Glaciology 41 (139): 455-464.

Cavalieri, D. J., J. Crawford, M. Drinkwater, W. J. Emery, D. T. Eppler, L. D. Farmer, M. Goodberlet, R. Jentz, A. Milman, C. Morris, R. Onstott, A. Schweiger, R. Shuchman, K. Steffen, C. T. Swift, C. Wackerman, and R. L. Weaver. 1992. NASA Sea Ice Validation Program for the DMSP SSM/I: Final Report. NASA Technical Memorandum 104559. National Aeronautics and Space Administration, Washington, D.C. 126 pages.

Cavalieri, D. J., J. Crawford, M. R. Drinkwater, D. Eppler, L. D. Farmer, R. R. Jentz and C. C. Wackerman. 1991. Aircraft Active and Passive Microwave Validation of Sea Ice Concentration from the DMSP SSM/I. Journal of Geophysical Research 96(C12):21,989-22,009.

Comiso, J. C. 1991. Satellite Remote Sensing of the Polar Oceans. Journal of Geophysical Research 2:295-434.

Comiso, J. C. 1990. Arctic Multiyear Ice Classification and Summer Ice Cover Using Passive Microwave Satellite Data. Journal of Geophysical Research 95(C8):13411-13422.

Comiso, J. C. 1986. Characteristics of Arctic Winter Sea Ice from Satellite Multispectral Microwave Observations. Journal of Geophysical Research 91(C1): 975-994.

Comiso, J. C. 1983. Sea Ice Effective Microwave Emissivities from Satellite Passive Microwave and Infrared Observations. Journal of Geophysical Research 88(C12):7686-7704.

Comiso, J. C., and C. W. Sullivan. 1986. Satellite Microwave and in-situ Observations of the Weddell Sea Ice Cover and its Marginal Ice Zone. Journal of Geophysical Research 91(C8):9663-9681.

Comiso, J. C., S. F. Ackley, and A. L. Gordon. 1984. Antarctic Sea Ice Microwave Signatures and Their Correlation with in-situ Ice Observations. Journal of Geophysical Research 89(C1):662-672.

Comiso, J. C., T. C. Grenfell, D. Bell, M. Lange, and S. Ackley. 1989. Passive Microwave in-situ Observations of Weddell Sea ice. Journal of Geophysical Research 88(C12):7686-7704.

Comiso, J. C., P. Wadhams, W. Krabill, R. Swift, J. Crawford, and W. Tucker. 1991. Top/Bottom Multisensor Remote Sensing of Arctic Sea Ice. Journal of Geophysical Research 96(C2):2693-2711.

Gloersen P. and D. J. Cavalieri. 1986. Reduction of Weather Effects in the Calculation of Sea Ice Concentration from Microwave Radiances. Journal of Geophysical Research 91(C3):3913-3919.

Gloersen P., W. J. Campbell, D. J. Cavalieri, J. C. Comiso, C. L. Parkinson, H. J. Zwally. 1992. Arctic and Antarctic Sea Ice, 1978-1987: Satellite Passive Microwave Observations and Analysis. NASA Special Publication 511.

Goodberlet, M. A. 1990. Special Sensor Microwave/Imager Calibration/Validation. Ph.D. dissertation submitted to the University of Massachusetts.

Grenfell, T. C. and J. C. Comiso. 1986. Multifrequency Passive Microwave Observations of First-year Sea Ice Grown in a Tank. IEEE Transactions on Geoscience and Remote Sensing GE-24:826-831.

Hollinger, J. P. 1989. DMSP Special Sensor Microwave/Imager Calibration/Validation. Naval Research Labs. Washington, D.C.

Hollinger, J. P. and R. C. Lo. 1983. SSM/I Project Summary Report. Naval Research Laboratory. NRL Memorandum Report 5055. 106 pp.

Hollinger, J. P., J. L. Pierce, G. A. Poe. 1990. SSM/I Instrument Evaluation. IEEE Transactions on Geoscience and Remote Sensing 28(5):781-790.

Hollinger, J. P., B. E. Troy, R. O. Ramseier, K. W. Asmus, M. F. Hartman, and C. A. Luther. 1984. Microwave Emission from High Arctic Sea Ice During Freeze-up. Journal of Geophysical Research 89(C5):8104-8122.

Hughes Aircraft Company. 1986. Data Requirements Document for Fleet Numerical Oceanography Center, Rev. B.

Hughes Aircraft Company. 1980. Special Sensor Microwave Imager (SSM/I), Computer Program Product Specification (Specification for FNMOC). Vol. II, Sensor Data Processing, Computer Program Component (SMISDP).

Martino, M. G., D. J. Cavalieri, and P. Gloersen. 1995 An Improved Land Mask for the SSM/I Grid. NASA Technical Memorandum TM104625.

Maslanik, J. A. 1992. Effects of Weather on the Retrieval of Sea Ice Concentration and Ice Type from Passive Microwave Data. International Journal of Remote Sensing 13(1):37-54.

Massom, R. A. 1991. Satellite Remote Sensing of Polar Regions. Boca Raton: Lewis Publishing.

Molthan, A. L., and M. R. Anderson. 2005. Locating and Removing Problematic Data in the DMSP SSM/I Data Sets. Abstract. 8th Conference on Polar Meteorology and Oceanography, 9-13 January 2005, San Diego, CA. View PDF.

Pearson, F. 1990. Map Projections: Theory and Applications. CRC Press. Boca Raton, Florida. 372 pages.

Poe, G. A. and R. W. Conway. 1990. A Study of the Geolocation Errors for the Special Sensor Microwave/Imager (SSM/I). IEEE Transactions on Geoscience and Remote Sensing 28(5):791-799.

Snyder, J. P. 1987. Map Projections - A Working Manual. U.S. Geological Survey Professional Paper 1395. U.S. Government Printing Office. Washington, D.C. 383 pages.

Snyder, J. P. 1982. Map Projections Used by the U.S. Geological Survey. U.S. Geological Survey Bulletin 1532.

Steffen, K. and A. Schwieger. 1991. NASA Team Algorithm for Sea Ice Concentration Retrieval from Defense Meteorological Satellite Program Special Sensor Microwave/Imager: Comparison with Landsat Satellite Imagery. Journal of Geophysical Research 96(C12):21,971-21,988.

Steffen, K., D. J. Cavalieri, J. C. Comiso, K. St. Germain, P. Gloersen, J. Key, and I. Rubinstein. 1992. The Estimation of Geophysical Parameters Using Passive Microwave Algorithms. Chapter 10 In Microwave remote sensing of sea ice. Frank Carsey, editor. American Geophysical Union. Washington, D.C. 243-259.

Stroeve, J. 1998. Impact of Various Processing Options on SSM/I-derived Brightness Temperatures. NSIDC Special Report-7.

Svendsen, E., K. Kloster, B. Farrelly, O. M. Johannessen, J. A. Johannessen, W. J. Campbell, P. Gloersen, D. Cavalieri, and C. Matzler. 1983. Norwegian Remote Sensing Experiment: Evaluation

of the Nimbus 7 Scanning Multichannel Microwave Radiometer for Sea Ice Research. Journal of Geophysical Research 88(C5):2781-2791.

Swift, C. T., D. J. Cavalieri. 1985. Passive Microwave Remote Sensing for Sea Ice Research. EOS 66(49):1210-1212.

Swift, C. T., Fedor, L. S. and Ramseier, R. O. 1985. An Algorithm to Measure Sea Ice Concentration with Microwave Radiometers. Journal of Geophysical Research 90(C1):1087-1099.

Wadhams, P., M. A. Lange, and S. F. Ackley. 1987. The Ice Thickness Distribution Across the Atlantic Sector of the Antarctic Ocean in Midwinter. Journal of Geophysical Research 92(C13):14,535-14,552.

Wentz, F. J. 1993. User's Manual: SSM/I Antenna Temperature Tapes. Rev. 2. Remote Sensing Systems, Inc. Santa Rosa, CA. RSS Technical Report 120193.

Wentz, F. J. 1992. Final Report, Production of SSM/I Data Sets. Remote Sensing Systems, Inc., Santa Rosa, CA. RSS Technical Report 090192.

Wentz, F. J. 1991. User's Manual: SSM/I Antenna Temperature Tapes. Remote Sensing Systems, Inc., Santa Rosa, CA. RSS Technical Report 032588.

4.1 Related Data Collections

Bootstrap Sea Ice Concentrations from Nimbus-7 SMMR and DMSP SSM/I
ESMR Polar Gridded Brightness Temperatures and Sea Ice Concentrations
Near-Real-Time DMSP SSM/I-SSMIS Daily Polar Gridded Brightness Temperatures
Near-Real-Time DMSP SSM/I-SSMIS Daily Polar Gridded Sea Ice Concentrations
Nimbus-7 SMMR Polar Gridded Radiances and Sea Ice Concentrations
DMSP SSM/I-SSMIS Pathfinder Daily EASE-Grid Brightness Temperatures
Sea Ice Concentrations from Nimbus-7 SMMR and DMSP SSM/I-SSMIS Passive Microwave Data
Sea Ice Trends and Climatologies from SMMR and SSM/I-SSMIS

5 CONTACTS AND ACKNOWLEDGMENTS

Roger Barry, Jim Maslanik, Walt Meier, Julienne Stroeve, Vince Troisi
National Snow and Ice Data Center (NSIDC)
Cooperative Institute for Research in Environmental Sciences (CIRES)
University of Colorado
Boulder, CO 80309 USA

6 DOCUMENT INFORMATION

6.1 Publication Date

May 2002

6.2 Date Last Updated

17 February 2021